

## PROBING MOLECULAR SHOCKS WITH MILLIMETER AND NEAR-IR INTERFEROMETRIC IMAGING

ZHONG. WANG

*IPAC, 100 - 22 California Institute of Technology,  
Pasadena, CA 91125, U.S.A.*

MICHAEL G. BURTON

*Anglo-Australian Observatory,  
P.O. Box 296, Epping, NSW 2121, Australia*

**ABSTRACT** We make detailed comparison between the high resolution CO ( $J=2-1$ ,  $1-0$ ) maps obtained with the OVRO Millimeter Array and the  $2.12 \mu\text{m}$  H<sub>2</sub> ( $v=1-0$ ) S(1) multi-channel images obtained using a Fabry-Perot system with the UKIRT Infrared Array Camera. Both datasets cover an interstellar shockfront region in the vicinity of the Galactic supernova remnant IC 443, and provide complementary information of the strongly shocked molecular gas on scales of 0.01 pc and a few  $\text{km s}^{-1}$ . Combining our data with other atomic/molecular line probes, we find that a *combination of bow-shock and cloud internal shock* can best describe the interface between the supernova blast wave and pre-existing molecular clouds.

## INTRODUCTION

Shockwaves are ubiquitous in the interstellar medium (ISM) because of the predominantly low temperature. Strong shocks, especially those occurring in molecular clouds, often show bright emission lines in the infrared and sub-mm/mm wavelengths. These emissions are characterized by high spatial and velocity variabilities which bear important clues to the underlying physics. Obviously, interferometric observations are particularly well suited to study molecular shocks. We observed a well-known molecular shock front region in IC 443 in both the CO lines and the H<sub>2</sub> S(1) line. A channel-to-channel comparison of the images of these molecular line emissions provides an unique probe of the shock structure.

## OBSERVATIONS

The shock interaction region discussed here is located in the vicinity of IC 443, the centering position of our maps is at  $\alpha = 06^{\text{h}}14^{\text{m}}41.7^{\text{s}}$ ,  $\delta = 22^{\circ}22'40''$  (1950.0). Figure 1. shows the single-dish (Nobeyama 45m) CO spectra observed at this peak emission region. Also plotted are the profiles of the  $2.12 \mu\text{m}$  H<sub>2</sub> S(1) line and the 21cm HI line made by integrating the near-IR Fabry-Perot data (see below) and high resolution VLA data, respectively, of the same region.

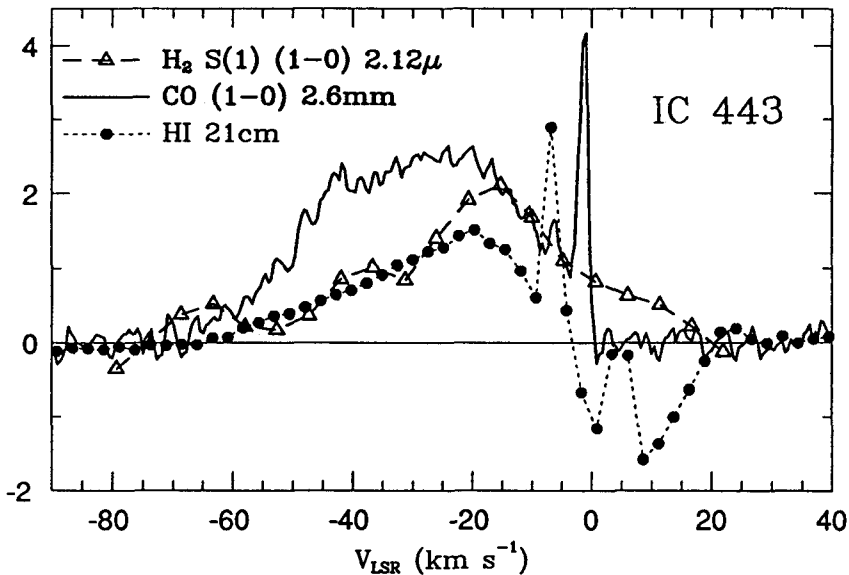


FIGURE 1 Spectral line profiles of CO, H<sub>2</sub>, and HI emission of a small region (see Figure 2) at the molecular shock front in IC 443. The H<sub>2</sub> data have some systematic variations due to incomplete background subtraction; while the HI emission suffers from absorption of foreground gas at near zero velocity. The vertical scales are arbitrary.

Our CO observations were made with the OVRO Millimeter array at 115 and 230 GHz, using a multi-field mosaicing technique. The configurations used are such that the resulting CO (2–1) and (1–0) images have comparable angular resolution of 3.5". The velocity resolution of the CO (1–0) image cube is 2.6 km s<sup>-1</sup>. More details of the observations are in Wang & Scoville (1992). The high resolution near-IR images were obtained using the UKIRT IR Camera with a FP system. They have a relatively small field of view of ~ 35" × 35", and a total of 20 consecutive wavelength settings were used, providing an effective velocity resolution of 5.33 km s<sup>-1</sup>. Figure II shows a comparison of the H<sub>2</sub> emission and CO (J=1–0) emission in nine velocity intervals, in which the channels of the OVRO data were binned to match that of the UKIRT data.

## RESULTS

- 1) the H<sub>2</sub> emission peaks in between the high (blueshifted) and low (redshifted) velocity CO emission regions at the shock front (see also Wang & Scoville 1992);
  - 2) the mean velocity of the H<sub>2</sub> emission is much redder than that of CO: most of the H<sub>2</sub> are found to correspond to the low velocity CO emission, or perhaps even redder;
  - 3) the H<sub>2</sub> emission is more compact than the CO in all velocity ranges; the high velocity CO appears more concentrated than its low velocity counterpart;
- In addition, comparisons with our VLA data suggest a close relationship between the high velocity atomic gas and the shocked molecular gas.

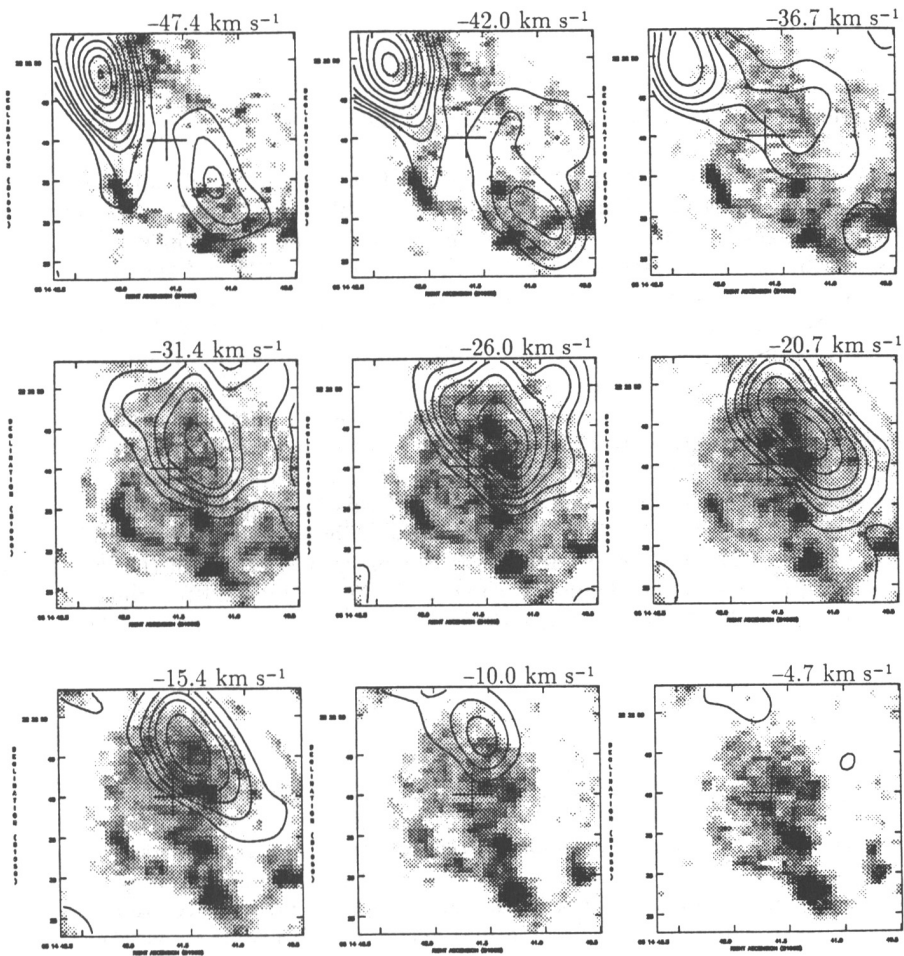


FIGURE II Channel-to-channel comparison of the ( $J=1-0$ ) CO data (contours), and the  $S(1)$  ( $v=1-0$ )  $H_2$  emission data (halftone). The  $H_2$  emission is seen in between the blue- and red-shifted CO emission, and is much brighter at the redshifted velocities. The region is about  $30''$  in size near a molecular shock front region in IC 443 (position C, see text). Each tickmark on the vertical (Declination) axes is  $5''$ . The positional accuracy of the overlay was estimated to be good to  $\pm 1''$ . Some low-level emission are seen as ring-like structures due to the incomplete continuum subtraction.

## INTERPRETATION

We find a detailed comparison of H<sub>2</sub> and CO channel maps to be helpful in constraining the available models of molecular shocks. For example, the data can rule out a scenario in which the shocked region consists of numerous cloudlets that are individually shocked, but are well-mixed as a whole. The clear morphological separation between the shock-heated hot gas (H<sub>2</sub>,  $T \simeq 2,000$  K) and the colder, CO-emitting gas implies that the molecular cloud shock has to occur coherently on scales of 0.05 pc or larger (at the assumed distance of 1.5 kpc for IC 443, 1'' corresponds to  $7 \times 10^{-3}$  pc).

In Wang & Scoville (1992), we proposed that the encounter of supernova blast waves with molecular clouds may create a combination of fast, dissociative J-shock and slow, continuous C-shock. In this view, the high velocity CO would be attributed to the fast shock, while the low velocity CO and the H<sub>2</sub> emission to the slow shock. If these two shocks are from two sides of a shock accelerated cloud, the observed morphology and kinematics can be accounted for naturally. However, this model may have some difficulties explaining the good correlation between the H<sub>2</sub> and HI emission.

An alternative interpretation of the present data is a model in which the CO emission mainly arises from a bow shock created by the supernova remnant, while the H<sub>2</sub> and HI emission come from a cloud internal shock that is of lower speed, but higher column density. Shocks of this kind have been predicted by McKee & Cowie (1975). The morphological differences between the high and low velocity CO emission are due to the line-of-sight effect when the bow shock is viewed from an angle behind, such that the highly blue-shifted component is more "edge-on" (Burton & Wang 1992).

## REFERENCES

- McKee, C. F., & Cowie, L. L. 1975, *ApJ*, **195**, 715  
 Wang, Z., & Scoville, N. Z. 1992, *ApJ*, **386**, 158  
 Burton, M. G., & Wang, Z. 1992, *in preparation*.

van der Werf: Can you elaborate on the correlation between H<sub>2</sub> and HI?

Wang: Yes, this can be seen in Figure I, where the HI profile shows reasonably good agreement with that of H<sub>2</sub> from the same region for  $v < -25$  km s<sup>-1</sup>. At more positive velocities the HI is contaminated by the foreground gas since IC 443 is almost at the Galactic anticenter direction. The HI profile in this figure differs from that of Wang & Scoville (1992) because now the VLA D-configuration data are included.

Genzel: What does the far-IR line emission, for example the [OI] line, tell you about the shocks in IC 443?

Wang: Pointing exactly at the same position as we discussed above, Burton *et al* (1990, *ApJ* 355, 197) discovered the [OI]63 $\mu$ m emission with the KAO. It has been shown that the line has to be shock excited and the preshock density is high. The emission is likely to be produced in C shocks, but could also be from a J shock under some special conditions.